NAT'L INST. OF STAND & TECH R.I.C.
A11105 654391

NIST
PUBLICATIONS

REFERENCE

NISTIR 6155

Analysis and Comparison of Various Image Downsampling and Unsampling Methods*

Abdou Youssef

Department of EECS
The George Washington University
Washington, D.C. 22052
youssef@seas.gwu.edu
Tel: (202) 994-6569
Fax: (202) 994-0227

*This research was performed in part at:

U.S. DEPARTMENT OF COMMERCE
Technology Administration
National Institute of Standards and Technology
Information Technology Laboratory
Gaithersburg, MD 20899

QC
100
.U56
NO.6155
1998

NIST

IPR2023-01014
Nielsen Company EX2023 Page 1

NISTIR 6155

Analysis and Comparison of Various Image Downsampling and Unsampling Methods*

Abdou Youssef

Department of EECS
The George Washington University
Washington, D.C. 22052
youssef@seas.gwu.edu
Tel: (202) 994-6569
Fax: (202) 994-0227

*This research was performed in part at:

U.S. DEPARTMENT OF COMMERCE
Technology Administration
National Institute of Standards and Technology
Information Technology Laboratory
Gaithersburg, MD 20899

December 1998

U.S. DEPARTMENT OF COMMERCE
William M. Daley, Secretary

TECHNOLOGY ADMINISTRATION
Gary R. Bachula, Acting Under Secretary for Technology

NATIONAL INSTITUTE OF STANDARDS AND TECHNOLOGY
Raymond G. Kammer, Director

Analysis and Comparison of Various Image Downsampling and Upsampling Methods[1]

Abdou Youssef
Department of EECS
The George Washington University
Washington, DC 20052
Tel: (202 994-6569, Fax: (202) 994-0227, Email: youssef@seas.gwu.edu

Abstract

Downsampling and upsampling are widely used in image display, and jointly used in compression and progressive transmission. In this paper we examine new down/upsampling methods using both frequency response analysis and experimental evaluation. Our findings show that *binomial* filters and some biorthogonal wavelet filters are among the best filters for down/upsampling, and significantly outperform the standard down/upsampling methods.

[1]This research was performed in part at the National Institute of Standards and Technology.

IPR2023-01014
Nielsen Company EX2023 Page 5

1 Introduction

Downsampling and upsampling are two fundamental and widely used image operations, with applications in image display, compression, and progressive transmission. Downsampling is the reduction in spatial resolution while keeping the same two-dimensional (2D) representation. It is typically used to reduce the storage and/or transmission requirements of images. Upsampling is the increasing of the spatial resolution while keeping the 2D representation of an image. It is typically used for zooming in on a small region of an image, and for eliminating the pixelation effect that arises when a low-resolution image is displayed on a relatively large frame.

More recently, downsampling and upsampling have been used in combination: in lossy compression [6], multiresolution lossless compression [1], and progressive transmission [2, 6]. In MPEG-2 video compression, the two color (chroma) components of every frame are downsampled by a factor of two before compression takes place; at reconstruction, the color components are upsampled back to their original 2D size. In multiresolution lossless compression, an image I is downsampled by a certain factor yielding an image D, and then D is upsampled by the same factor yielding an image I'; afterwards, both D and the residual image $R = I - I'$ are losslessly coded and stored. Clearly, the quality of the downsampling and upsampling methods has great impact on the performance (i.e., bitrate) of that compression scheme.

In progressive transmission, which has gained wide use on the Internet, the same downsample-upsample-residual coding method is used repeatedly to form a pyramid. Specifically, an image I_0 is downsampled by two repeatedly (say m times), yielding $I_1, I_2, \ldots, I_m$ (i.e., I_{i-1} is downsampled by two to yield I_i), then each I_i is upsampled by two to yield I'_{i-1}, and the residuals $R_i = I_i - I'_i$ are losslessly encoded to r_i and stored (note that $R_m = I_m$). When transmitting, r_m is sent first, then r_{m-1}, and so on. At the receiving end, r_m is decoded back to $R_m = I_m$ and displayed; then I_m is upsampled to I'_{m-1}, the just received r_{m-1} is decoded back to R_{m-1}, and $I_{m-1} = R_{m-1} + I'_{m-1}$ is computed and displayed; and so on. Here again, the quality of the down/upsampling methods has great impact on both the quality of the intermediate displays $I_m, I_{m-1}, ..., I_1$ and on the sizes (and thus transmission speed) of the r_i's.

The standard methods for downsampling are decimation and bilinear interpolation [6]. Decimation involves dropping every other row and every other column. Bilinear interpolation replaces every 2×2 window by its average pixel value when downsampling by two. The upsampling counterpart of decimation is duplication: it duplicates every row and every column. The upsampling counterpart of bilinear interpolation (called with the same name) inserts between every two pixels in a row (and column) the average value of the those pixels.

The increasing use of downsampling and upsampling, especially in combination, and the advent of new techniques such as wavelets [4, 8, 9], warrant a new and closer look into the methods of image downsampling and upsampling. Previous work dealing with down/upsampling [7, 3] predates wavelets and subband coding, and addresses general signal processing rather than focusing on visual signals (i.e., images) and related applications. Our goal is to gain a better understanding of the behavior of the image down/up-sampling processes, and, guided by that understanding, find better down/up-sampling methods than the ones currently used.

In this paper, we examine the existing methods and propose new methods of down/upsampling. We formulate a frequency-response approach for understanding and evaluating down/upsampling-combination methods. The approach is validated experimentally by running the examined methods on several different images and computing the signal-to-noise ratio (SNR) between the original and the down-then-upsampled image. The frequency-response-

IPR2023-01014
Nielsen Company EX2023 Page 6

based evaluation correlates well with the experimental evaluation.

Besides the standard methods mentioned above, we examine four classes of finite impulse response (FIR) filters for down/upsampling. The first two are the biorthogonal and orthogonal wavelets [4, 9]. The third class is what is termed here *binomial filters*. The fourth is the class of least-square filters [5], chosen from among the standard and optimal FIR filters.

Based on the proposed approach and the experimental validation, we identified the best down/upsampling-combination methods out of the several classes of methods that we investigated. Our findings show that the best down/upsampling filters are the binomial filters and some well-chosen biorthogonal wavelets. Bilinear interpolation was found significantly inferior, and decimation/duplication came last. Besides their superior SNR performance, binomial filters offer the added advantage of having rational coefficients with powers of two denominators — this improves the computational efficiency on many digital signal processors (DSP).

2 Formulation of the Down/Upsampling Process and Evaluation Approach

Consider a signal $x = (x_n)$. Downsampling x by two can be generally viewed as pre-filtering x with a linear filter $g = (g_k)$, yielding a signal $u = (u_n)$, and then decimating u by two, getting a signal $v = (v_n)$ where $v_n = u_{2n}$ for all n. Upsampling v by two, on the other hand, can be viewed as zero-upsampling followed by post-filtering. That is, v is zero-upsampled to a signal $w = (w_n)$ where $w_{2n} = v_n$ and $w_{2n+1} = 0$ for all n; then w is passed through a filter p yielding an approximation $\hat{x}$ of the original signal x. This general down/upsampling scheme, which is the low-pass half of the multirate subband coding scheme [8, 9], is shown in Figure 1. Note that in the case of 2D images, the downsampling is applied row-wise then column-wise, and the upsampling column-wise then row-wise. Note also that this general scheme captures the standard bilinear interpolation and decimation/duplication methods; their filters as well as other classes of filters will be presented in the next section.

Figure 1: **The General Downsampling/Upsampling Scheme**

To understand the behavior of the scheme, we use the z-transform (i.e., frequency-domain analysis). For any sequence $a = (a_n)$, be it a signal or a filter, the z-transform of a is a complex function $A(z) = \sum_n a_n z^n$. The z-transforms of x, u, v, w, $\hat{x}$, g and p, will be denoted $X(z)$, $U(z)$, $V(z)$, $W(z)$, $\hat{X}(z)$, $G(z)$ and $P(z)$, respectively. Note that we can and will limit z to the unit circle, i.e., $z = e^{i\omega}$, where ω is the frequency variable; $A(e^{i\omega})$ is the Fourier transform of a, and is thus periodic with period 2π, and its magnitude is symmetric around the origin.

We now derive the z-transform relation of the down/upsampling scheme of Figure 1. By the fundamental convolution theorem, $U(z) = G(z)X(z)$ and $\hat{X}(z) = P(z)W(z)$. Furthermore, $W(z) = \sum_n w_n z^n = \sum_n w_{2n} z^{2n} + \sum_n w_{2n+1} z^{2n+1} = \sum_n v_n z^{2n} = \sum_n u_{2n} z^{2n} = \frac{1}{2}[U(z) + U(-z)]$, using the facts that $w_{2n+1} = 0$, $w_{2n} = v_n = u_{2n}$. Consequently,

IPR2023-01014
Nielsen Company EX2023 Page 7

$$\hat{X}(z) = P(z)W(z) = \tfrac{1}{2}P(z)[U(z) + U(-z)] = \tfrac{1}{2}P(z)[G(z)X(z) + G(-z)X(-z)],$$

yielding

$$\hat{X}(z) = [\frac{1}{2}P(z)G(z)]X(z) + [\frac{1}{2}P(z)G(-z)]X(-z). \quad (1)$$

The first term on the right hand side of equation (1) is what contributes to the true reconstructed signal, while the second term is aliasing distortion. A good down/upsampling scheme yields a reconstructed signal $\hat{x}$ that is very close to the original signal x, and in the ideal (though impossible) extreme, $\hat{x} = x$, or correspondingly $\hat{X}(z) = X(z)$, for any input signal x. Equation (1) reveals that to have an ideal scheme, the filters g and p must satisfy the two identities $P(z)G(z) = 2$ and $P(z)G(-z) = 0$, which is clearly impossible. Nevertheless, knowing what is desired serves as a yardstick for comparative evaluation of candidate schemes. More importantly, equation (1), along with the understanding of the relevant characteristics of both the human visual system and typical natural images, will help us identify the desirable and more or less achievable properties of the two filters g and p of the scheme.

The preceding discussion shows that we must have $|P(z)G(-z)|$ as close to zero as possible, and $P(z)G(z)$ as close to 2 as possible. It is well-known that the human visual system is most sensitive to low-frequency (i.e., low-variation) signals, and that this sensitivity decreases quickly at higher frequencies (i.e., high-variation data). Therefore, it is desirable to have $P(z)G(z)$ very close to 2 in the largest low-frequency range possible, while still keeping $|P(z)G(-z)|$ near zero in the entire range of frequencies. In other terms, $P(z)G(z)$ should form a low-pass filter. In particular, g and p should be low-pass filters in their own right, especially when the downsampling and upsampling are to be used as two separate standalone operations and not just in combination. Fortunately, natural images contain largely low-frequency data, and thus the data loss incurred by such a scheme tends to be mathematically small and visually acceptable. It remains to determine how large we can make the low-pass band where $P(e^{i\omega})G(e^{i\omega})$ is near 2. This is addressed next.

Let g and p be two ideal low-pass filters, where $|G(e^{i\omega})|$ is 1 over $[0\ \alpha]$ and zero over $(\alpha\ \pi]$ for some α, and $|P(e^{i\omega})|$ is 2 over $[0\ \beta]$ and zero over $(\beta\ \pi]$ for some β. Observe that $|G(-z)| = |G(e^{i(\omega-\pi)})| = |G(e^{i(\pi-\omega)})|$ (because of the magnitude symmetry); therefore, $|G(-z)|$ is 1 over $[\pi - \alpha\ \pi]$ and 0 over $[0\ \pi - \alpha)$. Consequently, $|P(z)G(-z)|$ is 2 in the frequency range $[\pi - \alpha\ \beta]$ and zero in the remainder of $[0\ \pi]$. Since the ideal value of $|P(z)G(-z)|$ is zero over all $[0\ \pi]$, it follows that we should ideally have $\pi - \alpha \geq \beta$, that is, $\alpha + \beta \leq \pi$. On the other hand, $P(z)G(z)$ is 2 in the frequency range $[0\ min(\alpha, \beta)]$, and so $min(\alpha, \beta)$ is desired to be as large as possible. Clearly, when $\alpha + \beta \leq \pi$, the maximum value of $min(\alpha, \beta)$ is $\frac{\pi}{2}$, achieved at $\alpha = \beta = \frac{\pi}{2}$. We have thus proved the following theorem.

Theorem 1 *The ideal down/upsampling scheme is one where both filters g and p are low-pass filters with pass-band equal to $[0\ \frac{\pi}{2}]$. In that scheme, the aliasing distortion is zero, and the reconstructed signal preserves the largest possible range of low frequencies.*

Ideal low-pass filters are not achievable, especially with finite-length filters, but many families of finite filters approximate ideal filters reasonably well. With realistic low-pass filters g and p, $|P(z)G(z)|$ is approximately 2 in the frequency range $[0\ \frac{\pi}{2}]$ and approximately zero in $(\frac{\pi}{2}\ \pi]$, and $|P(z)G(-z)|$ is nearly zero throughout the frequency range $[0\ \pi]$ except for a "hump" around the middle of that range. Clearly, the smaller and narrower that hump is, the better. Those two yardsticks will be the basis of our evaluation of various filters for down/upsampling.

IPR2023-01014
Nielsen Company EX2023 Page 8

3 The Classes of Filters to Be Considered

We consider six classes of filters for down/upsampling. An important defining element for biorthogonal wavelets and binomial filters is the trigonometric polynomial

$$R_N(e^{i\omega}) = cos^{2N}(\frac{\omega}{2}) \sum_{k=0}^{N-1} \begin{pmatrix} N-k+1 \\ k \end{pmatrix} sin^{2k}(\frac{\omega}{2}),$$

for any positive integer N. The six classes of filters are:

- Biorthogonal wavelets [4]: Their filters g and p are characterized by $P(e^{i\omega})G(e^{i\omega}) = R_N(e^{i\omega})$, for $N \geq 1$. The combined length of g and p is $4N$.
- Binomial filters: They are characterized by $P(e^{i\omega}) = 2G(e^{i\omega}) = 2R_N(e^{i\omega})$, for $N \geq 1$. The filters g and p are symmetric of effective length $2N+1$ each (see Remark 1 below).
- Orthogonal wavelets: Daubechies well-known wavelets D_N [4]. The filters g and p are the length-N low-pass analysis and synthesis filters of D_N.
- Least-Square filters [5]: $p = 2g$ where g is a symmetric low-pass filter with cutoff at $\frac{\pi}{2}$.
- Bilinear interpolation: $g_{-1} = g_0 = 1/2$, $p_0 = 1$, $p_1 = p_{-1} = 1/2$. Undefined g_k & p_k are 0.
- Decimation/duplication: $g_0 = 1$, and $p_0 = p_1 = 1$. All undefined g_k and p_k are 0.

Remark 1: Because $cos^2(\frac{\omega}{2}) = z^{-1}(\frac{z+1}{2})^2$ and $sin^2(\frac{\omega}{2}) = -z^{-1}(\frac{z-1}{2})^2$, and because the coefficients of R_N are integers, it follows directly that the coefficients of g (i.e., the $4N-1$ coefficients of the Laurent polynomial $R_N(z)$ for $z = e^{i\omega}$) are all integers divided by powers of 2. This makes filtering an integer arithmetic process because division by a power of two is equivalent to shifting the binary representations. Furthermore, it can be shown that $R_N(-z) + R_N(z) = 1$ for all z on the unit circle. This implies that $g_0 = \frac{1}{2}$, $g_k = 0$ for all even nonzero indices k, and $g_{-k} = g_k$ for all k (i.e., g is symmetric around 0). In particular, the effective length of g, that is, the number of nonzero coefficients of g, is $2N+1$ rather than $4N-1$. Henceforth, a binomial filter will be denoted as "BN n", where n designates the effective length.

4 Frequency-Response Evaluation of the Six Classes

In this section the dual frequency responses $P(z)G(z)$ and $|P(z)G(-z)|$ of the six classes are evaluated and plotted in Figure 2, where $z = e^{i\omega}$ in the frequency range $[0\ \pi]$.

The biorthogonal wavelets form a large class since for any N there are many ways of factoring R_N into G and P, yielding filters of combined length $4N$. We generated all possible factorizations for all $N = 2, 3, ..., 14$, resulting in 4297 filter pairs (g, p). We measured the closeness of their frequency response to that of the ideal low-pass filter with passband $[0\ \pi/2]$, and accordingly selected the best 18 wavelets [10] (the majority of the other wavelets have poor frequency response). In this research, we evaluated the dual frequency responses of those 18 filter pairs; they all have good dual frequency responses, which improve as N increases. We

IPR2023-01014
Nielsen Company EX2023 Page 9

selected three filter pairs for our presentation (2nd row of Fig. 2): a min-length filter pair 9/7 (i.e., length(g)=9 and length(p)=7), a mid-length pair 16/16, and a max-length pair 33/19.

The class of binomial filters is very good and exhibit a consistent improvement in its dual frequency responses as N increases. We tested many members of this class, but we present here (1st row in Fig. 2) three binomial filter pairs (BN 7/BN 7, BN 15/BN 15 and BN 27/BN 27) whose lengths are comparable to the three biorthogonal filters chosen above; to simplify the comparison. As is evident in the Figure, the binomial filters have the best dual responses among all the classes considered, and the responses approach the ideal quickly as N increases.

The Daubechies orthogonal filter pairs also exhibit a consistent improvement in its dual frequency responses as N increases. Again, we chose three members (D_8/D_8, D_{16}/D_{16} and D_{28}/D_{28}) of lengths comparable to those chosen from the other classes. Note that although the dual response of D_N approaches the ideal as N increases, the orthogonal filters are not linear phase (unlike all the other classes considered). Therefore, they incur phase distortion which becomes worse for larger N. This will be evident in the experimental evaluation.

The dual responses of least-square (LS) filters also approach the ideal as the filter length increases. However, for reasonably short filters, the frequency response is quite far from ideal, and exhibits familiar ripples which increase in number as the filter length increases. We chose LS 8/LS 8, LS 16/LS 16, and LS 26/LS 26 for further evaluation (4th row of Fig. 2).

Finally, the dual frequency responses for bilinear interpolation and for decimation/duplication, shown the in the last row of Figure 2, are quite far from ideal, and very inferior to the first 5 classes. The decimation/duplication is the worst, especially with respect to its aliasing frequency response. The visual effect of that is the highly visible pixelation.

5 Experimental Evaluation and Validation

To validate our dual frequency response evaluation approach, and to get a quantified measure of the performance of the six classes, we tested them on two different images: the well-know image of Lena, and a fingerprint image. The test was carried out with three down/upsampling factors, 2, 4 and 8, where for 4 and 8 the downsampling (and upsampling) by two was performed twice and three times, respectively. For each filter pair and each sampling factor, the SNR between the original image and the down-then-upsampled image was computed.

The experimental results, both in objective SNR plots and in visual form as shown in Figures 3-9, are in agreement with the dual frequency response evaluation. The SNR plots show that the binomial filters and the selected biorthogonal wavelets are the best. The orthogonal filters perform well for short filters, but with long filters the phase distortion deteriorates the performance. Least-square filters perform poorly at short lengths, but improve significantly at higher length. The standard techniques, bilinear interpolation and decimation/duplication perform poorly — they are inferior to the binomial filters by about 4 and 6 decibels, respectively, which is significant.

Considering the efficiency importance of short-length filters, we examined the effect of filter length on performance within each of the first four classes. We added BN 5 in our testing because of the superior performance of binomial filters. Figure 4 gives four subfigures, where each subfigure plots the performance (on Lena) of several filter pairs of various lengths within one single class. The plots clearly show that for the two winning classes, binomial and biorthogonal, the length hardly matters, thus favoring short filters without much performance loss. For the

IPR2023-01014
Nielsen Company EX2023 Page 10

other two classes, orthogonal and least-square, the length has a big effect.

Figures 5-9 show visually the performance of decimation/duplication, bilinear interpolation, and binomial filters of effective length 9, on the image Lena, with 5 sampling factorsa (2, 4, 8, 16, and 32). It can be clearly seen that Binomial filters are superior, especially at sampling factors greater than 2.

We conclude by giving the coefficients of the winner filters in Tables 1, 2 and 3.

BN† 5: $g_0 = \frac{16}{2^5}$, $g_{\pm 1} = \frac{9}{2^5}$, $g_{\pm 3} = \frac{-1}{2^5}$
BN 7: $g_0 = \frac{256}{2^9}$, $g_{\pm 1} = \frac{150}{2^9}$, $g_{\pm 3} = \frac{-25}{2^9}$, $g_{\pm 5} = \frac{3}{2^9}$
BN 15: $g_0 = \frac{8388608}{2^{24}}$, $g_{\pm 1} = \frac{5153148}{2^{24}}$, $g_{\pm 3} = \frac{-1288287}{2^{24}}$, $g_{\pm 5} = \frac{429429}{2^{24}}$, $g_{\pm 7} = \frac{-122694}{2^{24}}$ $g_{\pm 9} = \frac{26026}{2^{24}}$, $g_{\pm 11} = \frac{-3549}{2^{24}}$, $g_{\pm 13} = \frac{231}{2^{24}}$

† p is implicit: $p_k = 2g_k \ \forall k$. Also, $g_{2k} = 0$ for all nonzero integers k.

Table 1: Three Binomial Filters

9/7 wavelet: $g_{-k} = g_k$ and $p_{-k} = p_k$								
$g_{0..4}$:	0.602949	0.266864	-0.078223	-0.016864	0.026749			
$p_{0..3}$:	1.115087	0.591272	-0.057544	-0.091272				
16/16 wavelet: $g_{-k} = g_{k-1}$ and $p_{-k} = p_{k+1}$								
$g_{0..7}$:	0.509000	0.036221	-0.094339	0.040131	0.027620	-0.017637	-0.003759	0.002763
$p_{1..8}$:	0.939274	0.265629	-0.162821	-0.089211	0.031598	0.020993	-0.003148	-0.002314
33/9 wavelet: $g_{-k} = g_k$ and $p_{-k} = p_k$								
$g_{0..16}$:	0.535998	0.300982	-0.040128	-0.071851	0.033196	0.026008	-0.017695	-0.007066 0.008725
	0.002367	-0.002558	-0.000504	0.000523	0.000068	-0.000065	-0.000003	0.000004
$p_{0..4}$:	0.043307	0.033844	-0.154696	-0.072745	0.622617			

Table 2: Filter Coefficients of Three Good Biorthogonal Wavelets

$D_8^{\ddagger}$ ($g_{0..7}$):	0.162902	0.505473	0.446100	-0.019788	-0.132254	0.021808	0.023252	-0.007493
D_{16} ($g_{0..15}$):	0.038478	0.221234	0.477743	0.413908	-0.011193	-0.200829	0.000334	0.091038
	-0.012282	-0.031175	0.009886	0.006184	-0.003444	-0.000277	0.000478	-0.000083

‡ p is implicit: $p_k = 2g_{-k+1} \ \forall k$.

Table 3: Two Orthogonal Daubechies Filters

IPR2023-01014
Nielsen Company EX2023 Page 11

6 Conclusions

In this paper we examined several classes of filters for down/upsampling, and found that binomial filters and certain biorthogonal filters are best. Considering also the short length and integer processing afforded by high-performance binomial filters, our single most important conclusion is that short-length binomial filters (5 or 7 coefficients) are the best choice. They can be used effectively in progressive transmission of images. They could also be used in variable-bandwidth video transmission as well as in prediction-based lossless compression. The latter two applications need further study, and are the subject of future research.

References

[1] S. R. Burgett and M. Das, "Multiresolution Multiplicative Autoregression Coding of Images," *Proc. IRRR Conference on Systems Engineering,* pp. 276–279, 1991.

[2] P. J. Burt and E. H. Adelson, "The Laplacian Pyramid as a Compact Image Code," *IEEE Transactions on Communications,* COM-31, pp. 532–540, Apr. 1983.

[3] R. E. Crochiere and L. R. Rabiner, *Multi-rate Digital Processing,* Prentice-Hall, 1983.

[4] I. Daubechies, *Ten Lectures on Wavelets,* Society for Industrial and Applied Mathematics, Philadelphia, 1992.

[5] L. B. Jackson, *Digital Filters and Signal Processing,* Kluwer Academic Publishers, 1996.

[6] "Generic Coding of moving pictures and associated audio (MPEG-2)", ISO-13818-2.

[7] R. W. Schafer and L. R. Rabiner, "A Digital Signal Processing Approach to Interpolation," *Proc. IEEE,* vol. 61, pp. 692–702, June 1973.

[8] P. P. Vaidayanathan, *Multirate Systems and Filter Banks,* Prentice Hall, 1993.

[9] M. Vetterli and J. Kovacevic, *Wavelets and Subband Coding,* Prentice Hall, 1995.

[10] A. Youssef, "Selection of Good Biorthogonal Wavelets for Data Compression," *International Conference on Imaging, Science, Systems, and Technology CISST '97,* Las Vegas, Nevada, pp. 323–330, June 1997.

IPR2023-01014
Nielsen Company EX2023 Page 12

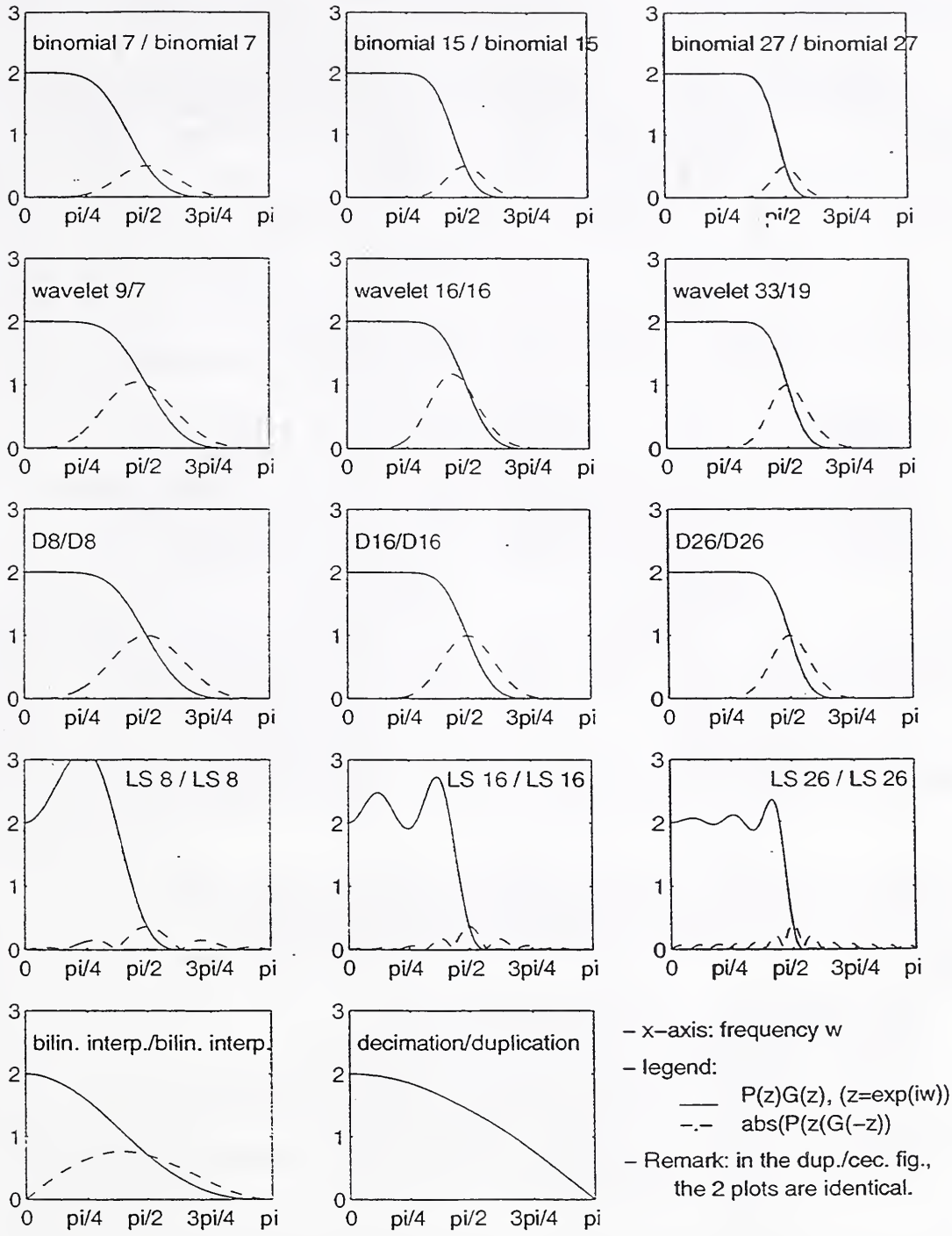

Figure 2: The Frequency Response of Down/Upsampling Scheme for the Six Classes of Filters

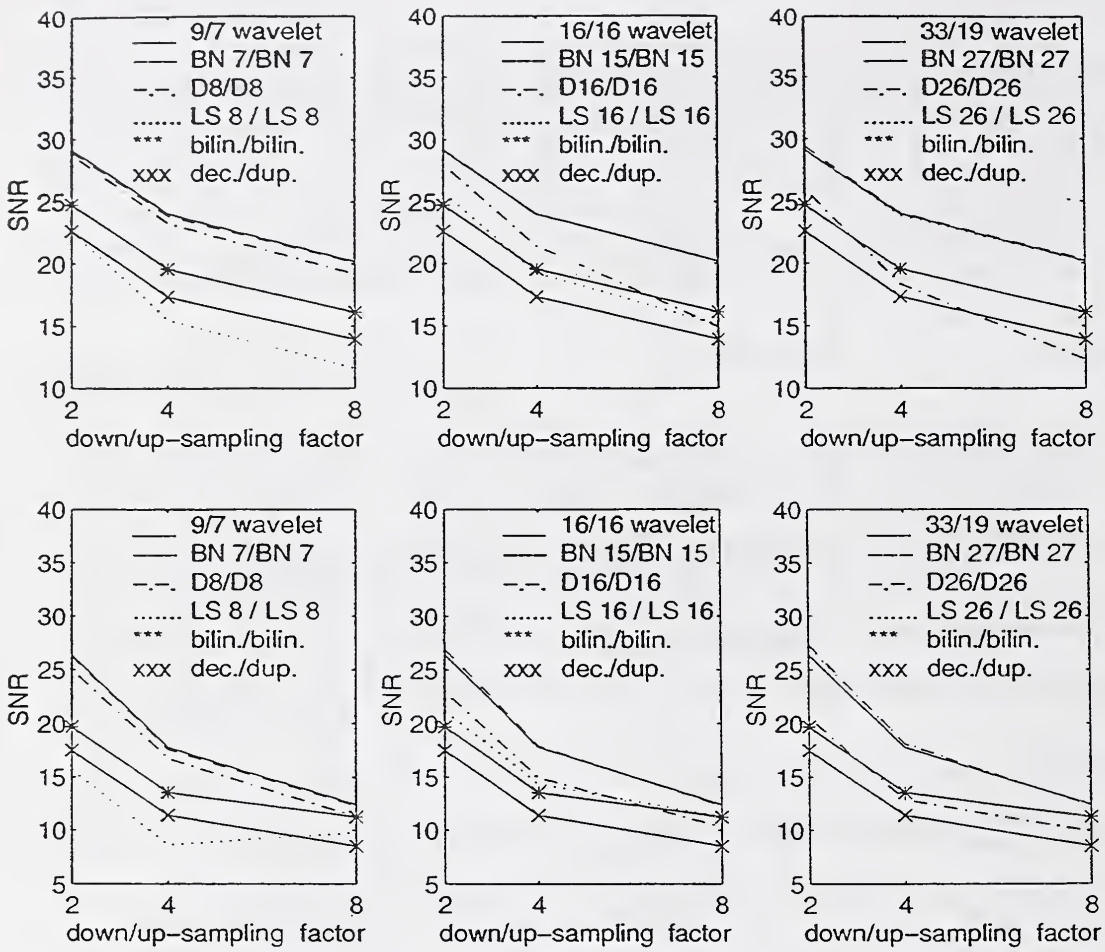

– These figures plot the SNR at 3 sampling factors for various filters of various lengths

– The top row of plots is generated from running the scheme on the image Lena

– The bottom row of plots is generated from running the scheme on a fingerprint image

– Notation:

BN=binomial; D=Daubechies; LS=least–square filters;

bilin.=bilinear interpolation; dec.=decimation; dup.=duplication

X/Y designates that the downsampling filter is X and the upsampling filter is Y

n/m wavelet refers to the biorthogonal wavelets in Table 1

– Remark: the bilin./bilin. and dec./dup. schemes are the same in the 3 plots of each row; they are repeated for clear comparison.

Figure 3: Experimental Evaluation of The Down/Upsampling Schemes

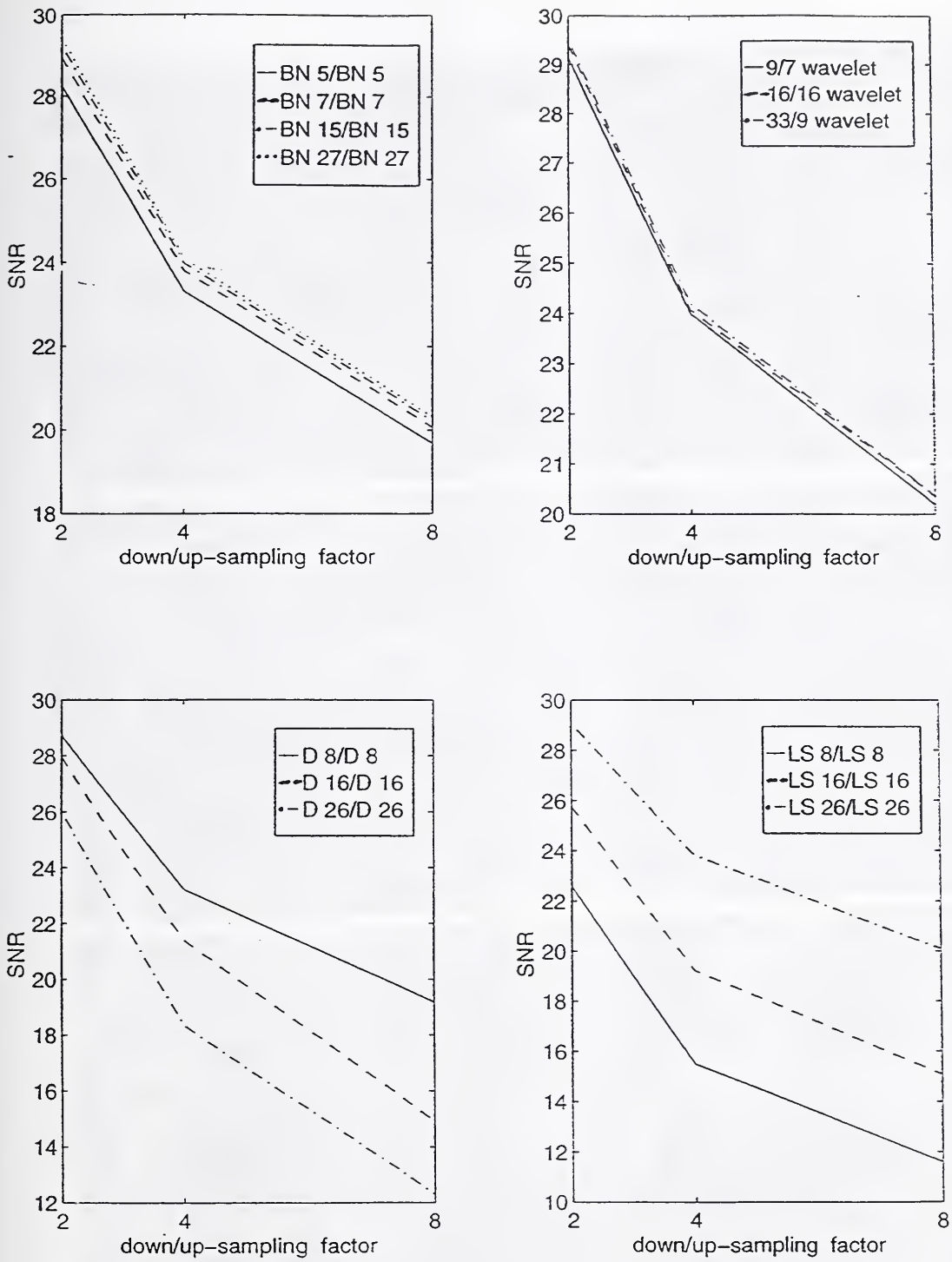

Figure 4: Impact of the Filter Length on the Performance of the First 4 Classes

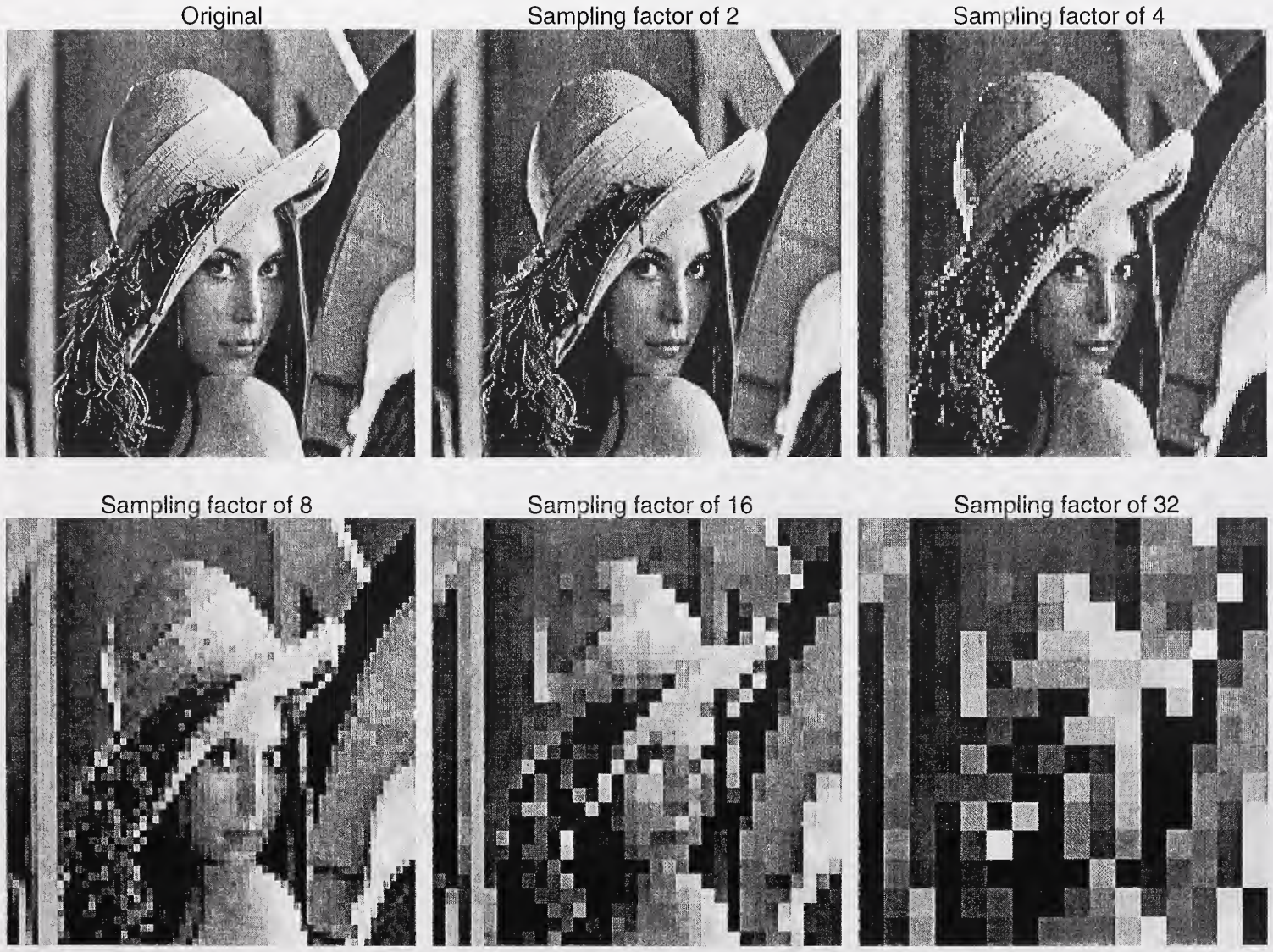

Figure 5: Downsampling by Decimation, Upsampling by Duplication

Figure 6: Downsampling and Upsampling by Bilinear Interpolation

Figure 7: Downsampling and Upsampling with a Binomial Filter of Effective Length 9

Figure 8: Comparison Between Binomial Filtering BN9 (Top) and Decimation/Duplication (Bottom)

Figure 9: Comparison Between Binomial Filtering BN9 (Top) and Bilinear Interpolation (Bottom)